Vol. **1**, **4**. 239-251 (2003)

Revue de Mécanique Appliquée et Théorique

Application of the Mechanical Threshold Stress for the analysis of the shear band spacing in HY-100 steel

O. Oussouaddi
LMCS, Department of Physics, FSTE, University Moulay Ismaïl, Errachidia, Morocco

L. Daridon
IMFS-UMR 7507 CNRS, University Louis Pasteur, IPST, Strasbourg, 67100, France

S. Ahzi
IMFS-UMR 7507 CNRS, University Louis Pasteur, IPST, Strasbourg, 67100, France

D. Bouami
LCE, Department of Mechanical Engineering, EMI, University Mohamed V, Morocco

Résumé

Cette étude est relative à l'analyse de la formation de bandes de cisaillement adiabatique multiples dans l'acier HY-100. On analyse, en cisaillement simple, par l'intermédiaire de critères analytiques et par calcul numérique l'instabilité et l'espacement entre bandes de cisaillement. Le modèle de contrainte seuil mécanique (Mechanical Threshold Stress (MTS)) a été adopté dans cette analyse. Le modèle MTS est basé sur l'utilisation de la contrainte seuil mécanique comme une variable d'état interne, qui décrit avec succès le comportement des métaux à grandes vitesses de déformation. Nous utilisons la méthode des perturbations pour analyser la stabilité d'une solution homogène des équations gouvernant le problème du cisaillement simple. la plus petite valeur de la déformation moyenne pour laquelle la solution homogène perturbée devient instable s'appelle la déformation critique ou déformation d'instabilité. Dans les quelques études qui existent dans ce domaine, la loi de puissance est largement utilisée et mène à une solution analytique du problème. Notre approche basée sur l'utilisation du modèle MTS nécessite une solution numérique des équations de la chaleur et de l'évolution de la variable interne. L'espacement entre bandes de cisaillement est calculé en utilisant le postulat de Wright et Ockendon. Ce postulat stipule que la longueur caractéristique du mode d'instabilité dominant ayant la vitesse de croissante maximale au temps t_0, détermine l'espacement minimal entre bandes de cisaillement. Les effets des paramètres du matériau et des conditions de chargement sur l'espacement entre bandes sont discutés. Les résultats obtenus avec le modèle MTS sont comparés avec ceux obtenus avec la loi puissance.

Abstract

This work concerns the analysis of the formation of multiple adiabatic shear bands in HY-100 steel. We analyze, via analytical criteria and numerical calculations, instability and shear band spacing in simple shear. The Mechanical Threshold Stress (MTS) model is used in our proposed analysis. The MTS model is based on the use of the mechanical threshold stress as an internal state variable, which successfully describes the deformation response of metals at high strain rates. We used the perturbation method to analyze the stability of a homogenous solution of the governing equations. The smallest value of the average strain for which the perturbed homogeneous solution becomes unstable is called the critical strain or instability strain. In the few existing works in this area, the power law is widely used and leads to analytical solution. The proposed approach based on the use of the MTS model requires numerical solution for the heat equation and the evolution equation of the

Received 23 July 2002
Revised 31 October 2002

internal variable. The shear band spacing is computed using Wright and Ockendon's postulate which suggests that the wavelength of the dominant instability mode with the maximum growth rate at time t_0 determines the minimum spacing between shear bands. The effects of material parameters and loading conditions on the shear band spacing are discussed. The results from the MTS model are compared to those of the power law based model.

1. INTRODUCTION

The localization of plastic deformation in narrow bands is a major damage mechanism that occurs in ductile materials during high strain rate deformation. They are observed in various applications such as metal forming, ballistic impact and high speed machining. Their formation signals a transition from a generally homogeneous deformation to a nonhomogeneous one involving high strain gradients in a narrow region. In some circumstances many small bands may form throughout a volume of material [1], in which case a general weakening occurs with the possibility of multiple failures and a general fragmentation. In other circumstances one band may dominate and material failure is restricted to just that one location. In the experiments of Marchand and Duffy [2], thin-walled tubes were twisted at nominal strain rates in the range of 1200 s^{-1} to 1600 s^{-1}. Only one shear band is observed in their specimen. However, during the radial collapse of thick-walled cylinder deformed at a strain rate of 10^4 s^{-1}, Nesterenko et al. [1] observed twenty shear bands spaced about 0.85 and 1 mm in titanium and austenitic stainless steel, respectively.

Few numerical studies of the shear bands spacing are available in the literature. Grady and Kipp [3] have obtained the shear band spacing by accounting for momentum diffusion due to unloading within bands. Wright and Ockendon [4] used a perturbation analysis to characterize a dominant mode which corresponds to the most probable minimum spacing of shear bands. Linear perturbation analysis which has been used in fluid mechanics, is first introduced in the context of adiabatic shear banding by Clifton [5], Bai [6], Molinari [7, 8], Shawki and Clifton [9] among others (e.g. see Bai and Dodd, [10]). Wright and Ockendon [4] postulated that, in an infinite body, perturbations growing at different sites will never merge and result in multiple shear bands. Thus, the wavelength of the dominant instability mode with the maximum initial growth rate will determine the shear band spacing. Molinari [11] has extended Wright and Ockendon [4] work to strain-hardening materials and has estimated the error in the shear band spacing due to the finite thickness of the block deformed in simple shear. Recently, Batra and Chen [12] showed that four viscoplastic relations (Wright-Batra, Johnson-Cook, power law, and Bodner-Partom relation) gave quite different values for the shear band spacing and the bandwidth.

In this paper, we adapted a three-term Mechanical Threshold Model (MTS) model, which includes the superposition of different thermal activation barriers for dislocation motion. In this model, evaluation of work hardening associated with dislocation accumulation and recovery is principally based on the Voce law. The MTS model is based on the dislocation concepts (Follansbee and Kocks [13]) which was originally developed by Mecking and Kocks [14]. This model provides a better understanding of the plastic behavior. The system of governing equations for one-dimensional simple shearing deformations is formulated. For a given value of the strain, a perturbation of the fundamental solution is considered and the instability modes are determined. We used the postulate of Wright and Ockendon to determine the shear band spacing. The effects of material parameters and the loading conditions on the shear band spacing are discussed. We compare the results from our proposed approach based on the MTS model with those obtained by using the viscoplastic power law. The considered material in this study is HY100 steel.

2. FORMULATION OF THE PROBLEM

Let us consider a simple shearing deformation of a plate with a finite thickness 2h in the y-direction whereas it is infinite in the other two rectangular cartesian directions (Figure 1). At the upper and lower surfaces, constant velocities $\pm V$ are applied parallel to the x-direction. We assume that all physical quantities are uniform along the x and z directions so that the deformation depends only on the space coordinate y.

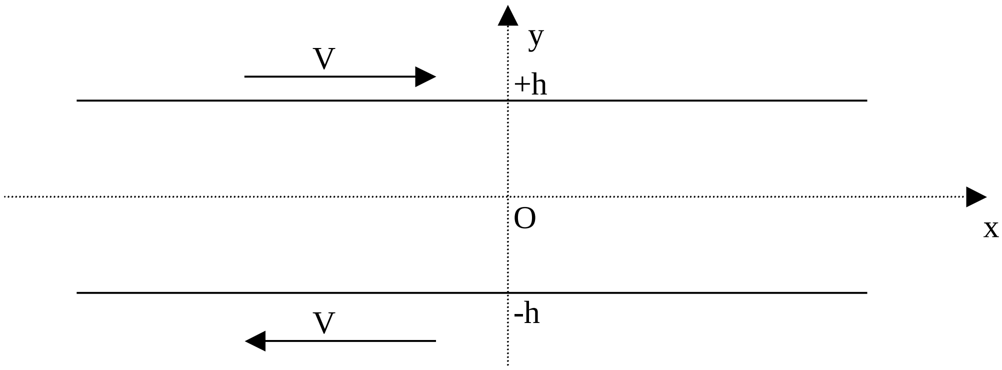

Figure 1: Geometry of the problem

In addition to the relation constitutive defined in the following paragraph, the equations governing the problem, when elastic strains are ignored are:

$$\rho \frac{\partial v}{\partial t} = \frac{\partial \tau}{\partial y} \tag{1}$$

$$\rho c \frac{\partial T}{\partial t} - k \frac{\partial^2 T}{\partial y^2} = \beta \tau \dot{\gamma} \tag{2}$$

$$\dot{\gamma} = \frac{\partial v}{\partial y} \tag{3}$$

$$\frac{d\phi}{d\gamma} = f(\phi, \tau, T, \dot{\gamma}) \tag{4}$$

where (1) is the momentum balance equation, (2) the energy equation, (3) the compatibility equation, and (4) gives the evolution of an internal variable ϕ (the form of the function f will vary with the used constitutive relation); with v, γ, τ and T being respectively, the particle velocity (in the y direction), the plastic shear strain, the shear stress and absolute temperature. The physical parameters ρ, c, k and β are the mass density, the specific heat, the heat conductivity and the Taylor-Quinney coefficient which represents the fraction of plastic work converted into heat, respectively. The value of these physical parameters are given in Table 1. A superimposed dot denotes the material time derivative.
As high strain rates are considered, adiabatic conditions can be assumed at the boundaries:

$$\frac{\partial T}{\partial y}(y=-h,t)=\frac{\partial T}{\partial y}(y=+h,t)=0 \tag{5}$$

Parameter	[Units]	Value
ρ	[kg/m^3]	7860
c	[J/kg.K]	473
k	[W/m^2.K]	49.73
β		0.9

Table 1. Physical parameters of HY-100 steel

3. VISCOPLASTIC RELATIONS

3.1 The Mechanical Threshold Stress model

The physically based MTS model is an isotropic scalar relation that expresses flow stress as a function of strain rate, temperature and current state (through a state variable called the mechanical threshold). The mechanical threshold, $\hat{\tau}$, is defined as the flow stress at 0 K. The model is used with some modifications depending on the material examined and is given in a general form for the HY-100 steel considered here, as:

$$\hat{\tau} = \hat{\tau}_a + \hat{\tau}_i + \hat{\tau}_\varepsilon \tag{6}$$

where $\hat{\tau}_a \equiv \tau_a$ is a minor contribution due to athermal strengthening, e.g. grain boundary, $\hat{\tau}_i$ characterizes the rate-dependent interactions of dislocations with short-range barriers due to solute and interstitial atoms and $\hat{\tau}_\varepsilon$ characterizes the rate-dependent interactions of dislocations with long-range barriers considering other dislocations and carbide particles. We note that $\hat{\tau}_\varepsilon$ is increased during deformation by increasing of dislocation density that depends on temperature and strain rate because dynamic recovery takes place.

At different temperatures T and shear strain rates $\dot{\gamma}$, the contributions to the flow shear stress τ_j are related to their reference counterparts $\hat{\tau}_j$ through the scaling functions $S_j(\dot{\gamma}, T)$ so that $\tau_j = S_j(\dot{\gamma}, T)\hat{\tau}_j$, where j = i or ε. Hence, the flow shear stress τ is described as follows:

$$\frac{\tau}{\mu} = \frac{\tau_a}{\mu} + S_i(\dot{\gamma}, T)\frac{\hat{\tau}_i}{\mu_0} + S_\varepsilon(\dot{\gamma}, T)\frac{\hat{\tau}_\varepsilon}{\mu_0}, \tag{7}$$

where μ_0 is the shear modulus at 0K and the dependence of the shear modulus μ on temperature is given by the following empirical relation [17, 18]:

$$\mu = \mu_0 - \frac{D}{\exp\left(\frac{T_0}{T} - 1\right)} \tag{8}$$

in which T_0 and D are empirical constants.

The scaling factor is derived from an Arrhenius expression relating strain rate to activation energy and temperature:

$$\dot{\gamma} = \dot{\gamma}_{0j} \exp\left(-\frac{\Delta G_j}{kT}\right), \quad \text{where } \Delta G_j = g_{0j}\mu b^3\left(1-\left(\frac{\tau_j}{\hat{\tau}_j}\right)^{p_j}\right)^{q_j}, \tag{9}$$

where $\dot{\gamma}_{0j}$ is a reference shear strain rate, k is the Boltzmann constant, T is absolute temperature, g_{0j} is a normalized activation energy and b is the Burgers vector and p_j and q_j are statistical constants that characterize the shape of the obstacle profile ($0 \le p_j \le 1,\ 1 \le q_j \le 2$), (Kocks et al. [16]). The scaling factor $S_j(\dot{\gamma}, T)$ can be derived from (9) as:

$$S_j(\dot{\gamma}, T) = \left\{1-\left[\frac{kT}{g_{0j}\mu b^3}\ln\left(\frac{\dot{\gamma}_{0j}}{\dot{\gamma}}\right)\right]^{1/q_j}\right\}^{1/p_j} \tag{10}$$

Plastic strain is implicitly represented through the term representing structure evolution $\hat{\tau}_\varepsilon$. The specific form for the expression of the plastic strain, γ, is dependent on the strain-hardening rate description. The strain-hardening response within the MTS model is given by Voce law as:

$$\theta = \frac{d\hat{\tau}_\varepsilon}{d\gamma} = \theta_0\left[1-\frac{\tanh\left(2\frac{\hat{\tau}_\varepsilon}{\hat{\tau}_{\varepsilon s}}\right)}{\tanh(2)}\right] \tag{11}$$

where $\hat{\tau}_{\varepsilon s}$ is a temperature and rate-sensitive saturation shear stress, and θ_0 is an experimentally determined stage II strain hardening rate. The dependence of θ_0 on temperature is determined by Goto et al. [15], $\theta_0 = 5102.4 - 2.0758 \times T\ [\mathrm{MPa}]$. The saturation stress $\hat{\tau}_{\varepsilon s}$ is derived from the saturation threshold stress $\hat{\tau}_{\varepsilon s0}$ by:

$$\ln\left(\frac{\dot{\gamma}_{\varepsilon s0}}{\dot{\gamma}}\right) = -\frac{g_{0\varepsilon s}\mu b^3}{kT}\ln\left(\frac{\hat{\tau}_{\varepsilon s}}{\hat{\tau}_{\varepsilon s0}}\right) \tag{12}$$

where $g_{0\varepsilon s}$ is normalized activation energy for dislocation-dislocation interactions.
The values of the material constants of the above described model are listed in Table 2, [15].

3.2 Power law

Molinari and Clifton [20], Klopp et al. [19], Marchand and Duffy [2], Batra et al. [12] and Molinari [7] have described the stress-strain curves for dynamic loading using a power law:

$$\tau = \tau_0 \left(\frac{\gamma}{\gamma_y} \right)^n \left(\frac{\dot{\gamma}}{\dot{\gamma}_0} \right)^m \left(\frac{T}{T_0} \right)^\nu \tag{13}$$

where γ_y is the strain at yield in a quasi-static simple shear test at $\dot{\gamma}_0 = 10^{-4}\,s^{-1}$, the parameters n and m characterize the strain and strain-rate hardening of the material and $\nu \langle 0$ is the thermal softening parameter. The material parameters have been identified in the work of Batra and Kim [21-23] by solving an initial-boundary-value problem that closely simulated the test conditions of Marchand and Duffy [2] and ensured that the computed stress-strain curve matched well the experimental data. Their values are:

$$\dot{\gamma}_0 = 10^{-4}\,s^{-1}, \gamma_y = 0.012, T_r = 300\,K, m = 0.0117, n = 0.107, \nu = -0.75.$$

For this case, $\phi = f = 0$.

Parameter	[Units]	Value	Parameter	[Units]	Value
τ_a	[MPa]	40 E+6	q_i		1.5
$\hat{\tau}_i$	[MPa]	1341E+6	p_i		0.5
μ_0	[MPa]	71460E+6	$\dot{\gamma}_{0\varepsilon}$	[s^{-1}]	1E+7
D	[MPa]	2910E+6	$g_{0\varepsilon}$		1.6
T_0	[K]	204	q_ε		1
k	[J/K]	1.38E-23	p_ε		2/3
b	[m]	2.48E-10	$g_{0\varepsilon s}$		0.112
$\dot{\gamma}_{0i}$	[s^{-1}]	1E+13	$\dot{\gamma}_{0\varepsilon s}$	[s^{-1}]	1E+7
g_{0i}		1.161	$\hat{\tau}_{\varepsilon s0}$	[MPa]	790E+6

Table 2: MTS model parameters for HY-100 steel [15]

4. PERTURBATION ANALYSIS

We consider a small perturbation of the homogeneous solution at time t_0 (the average strain at t_0 is given by $\gamma^0 = \dot{\gamma}^0 . t_0$) that evolves with time t:

$$\delta \mathbf{s}(y, t, t_0) = \delta \mathbf{s}^0 e^{\eta(t - t_0)} e^{i\xi y}, \; t \ge t_0 ; \tag{14}$$

where $\delta \mathbf{s}^0 = \left(\delta v^0, \delta\gamma^0, \delta\tau^0, \delta T^0 \right)$ and y represents the position along the thickness of the plate. The quantities $\delta v^0, \delta\gamma^0, \delta\tau^0, \delta T^0$ are small constants that characterize the initial amplitude (at time t_0) of the perturbation. ξ is the wave number of perturbation, and η is the rate of growth. The homogeneous solution is stable when the real part $R_e(\eta)$ is negative and is unstable when $R_e(\eta)$ is positive. The perturbation is added to the homogeneous solution which leads to:

$$\mathbf{s}(y,t,t_0) = \mathbf{s}^0(y,t) + \delta\mathbf{s}(y,t,t_0) \tag{15}$$

We substitute this perturbed solution into the governing equations (1-4) and (7) or (13) and then the linearization provides, at time t_0, a linear system of equations for the amplitude vector $\delta\mathbf{s}^0$:

$$\mathbf{A}(t_0,\eta,\xi).\delta\mathbf{s}^0 = 0 \tag{16}$$

The system of equations (16) has a nontrivial solution only if det (A)=0. This gives the following cubic equation for the growth rate η:

$$\rho^2 c\eta^3 + \rho\left(c\xi^2 \frac{\partial\tau}{\partial\dot{\gamma}}\bigg|_{s^0} + k\xi^2 - \beta\dot{\gamma}^0 \frac{\partial\tau}{\partial T}\bigg|_{s^0}\right)\eta^2 + \left(k\xi^2 \frac{\partial\tau}{\partial\dot{\gamma}}\bigg|_{s^0} + \rho c\left(f^0 \frac{\partial\tau}{\partial\phi}\bigg|_{s^0} + \frac{\partial\tau}{\partial\gamma}\bigg|_{s^0}\right) + \beta\tau^0 \frac{\partial\tau}{\partial T}\bigg|_{s^0}\right)\xi^2\eta +$$
$$k\left(f^0 \frac{\partial\tau}{\partial\phi}\bigg|_{s^0} + \frac{\partial\tau}{\partial\gamma}\bigg|_{s^0}\right)\xi^4 = 0 \tag{17}$$

where partial derivatives are evaluated for the fundamental solution at time t_0. For given values of γ^0 and ξ, the root η_D with the largest positive real part governs the instability of the homogeneous solution, and is hereafter referred to as the dominant instability mode.

The fundamental solution is such that the strain rate is uniform, $\dot{\gamma}^0 = \frac{V}{h}$. We note that in the case of power law, the heat equation (2) can be resolved analytically, with adiabatic assumption and where the constitutive law (13) is used to express the stress τ. However in the case of MTS model the temperature is obtained by numerical integration of the heat equation (2) and the evolution equation of the internal variable (4), and where the constitutive law (7) is used to express the stress τ.

5. RESULTS AND DISCUSSION

For the nominal strain-rate $\dot{\gamma}^0$ of 10^4 s^{-1}, Figure 2(a) shows the growth rate η_D at time t_0 (or at the average strain γ_0) versus the wave number ξ for five different values of the average strain γ^0 when the initial perturbation is introduced using the MTS model. Figure 2(b) shows the same results as Figure 2(a) for the power law model. The existence of a dominant mode results from the competition of two stabilizing effects. Inertia restrains the growth of long-wavelength modes (small ξ) while heat conduction restrains the growth of small-wavelength modes (large ξ). It is observed that the dominant growth rate increases with an increase in the wave number, attains a maximum value and then decreases. Henceforth, the maximum dominant growth rate at time t_0 for the perturbations is called the critical growth rate η_c, and the corresponding wave number is the critical wave number ξ_c.

Figures 3(a)-(b) show, for the nominal strain rate of $10^4\,s^{-1}$, the dependence of η_c and the corresponding wavelength $L_c = 2\pi/\xi_c$ on the average strain γ^0 for both the MTS and the power law models. We note that η_c is a function of the average strain γ^0. The average strain corresponding to the maximum value of η_c and the minimum value of L_c is 1.13 for the MTS model and 0.99 for the power law. Figure 4 evinces, for the two viscoplastic constitutive relations, the dependence upon the nominal strain rate of the average strain corresponding to the maximum growth rate of the perturbation. For the MTS model we note that the average strain corresponding to the maximum growth rate of the perturbation increases slightly with increasing nominal strain-rate. However, this average strain is essentially unchanged for the power law. This average strain does not varies with the thermal conductivity for both models.

It the case of non-hardening materials, Wright and Ockendon [4] postulated that the dominant instability mode with the maximum growth rate at time t_0 determines the shear band spacing, L_s. In this case, the critical value η_c is reached at the right beginning of loading process (i.e. at the initial time for $\gamma_0^c = 0$). For strain hardening materials, Molinari (1997) define precisely the concept of critical time of strain ($(t_0^c,\ \gamma_0^c)$ and postulated that the shear banding spacing is given by:

$$L_s = \frac{2\pi}{\xi_c(t_0^{\eta_c})} \tag{19}$$

where $t_0^{\eta_c}$ corresponds to the time when $\eta_c(t_0)$ is maximum.

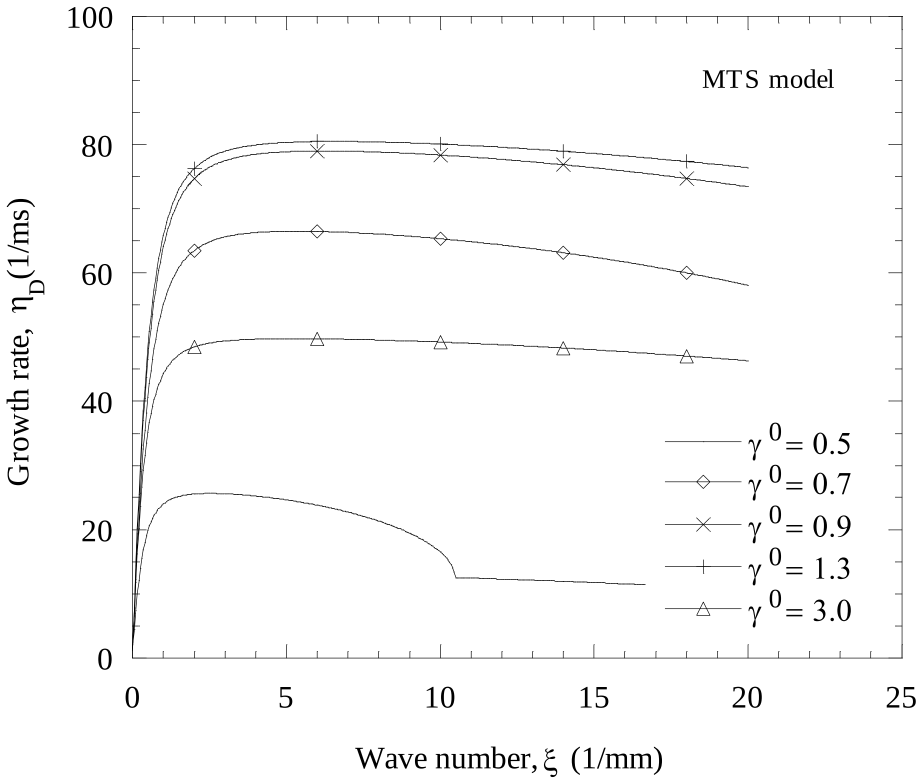

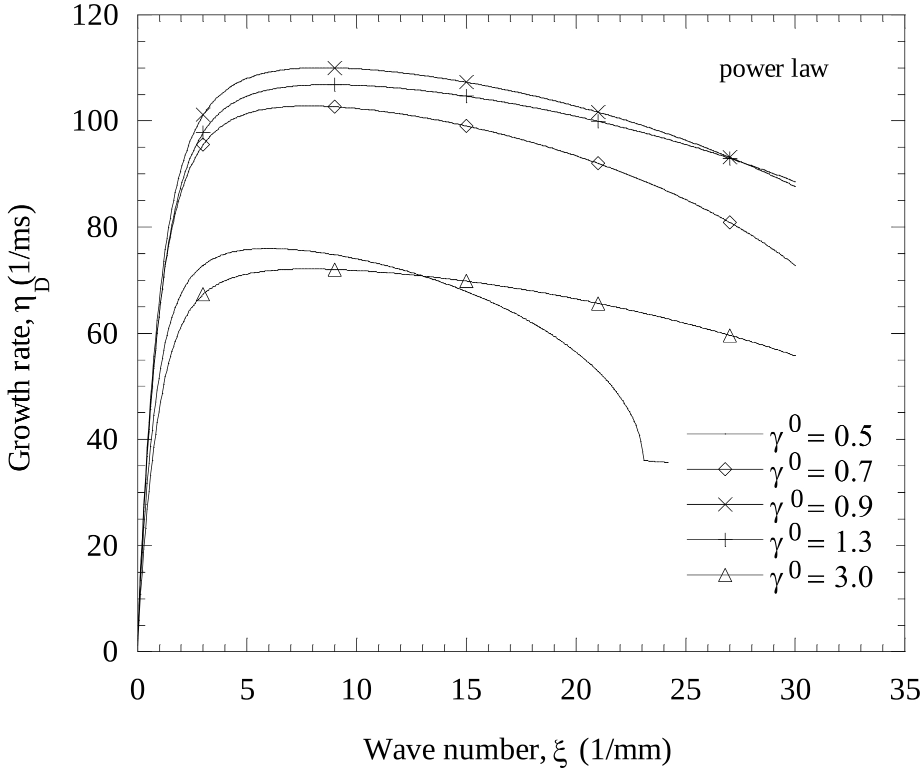

Figure 2: Growth-rate η_D versus the wave number ξ for five different value of the average strain, γ^0

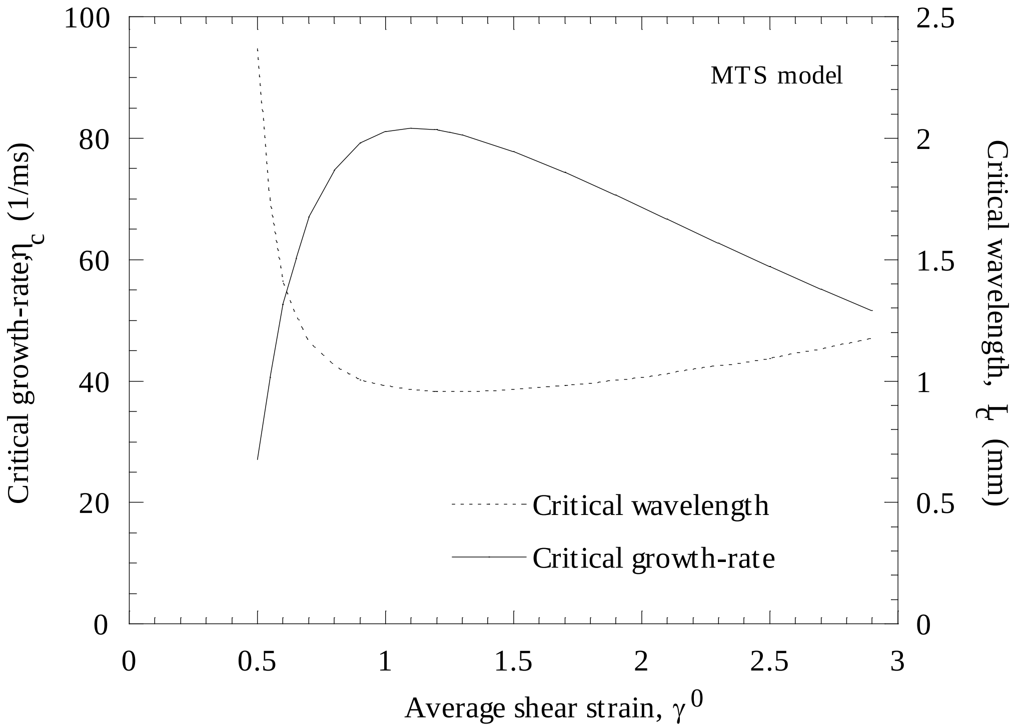

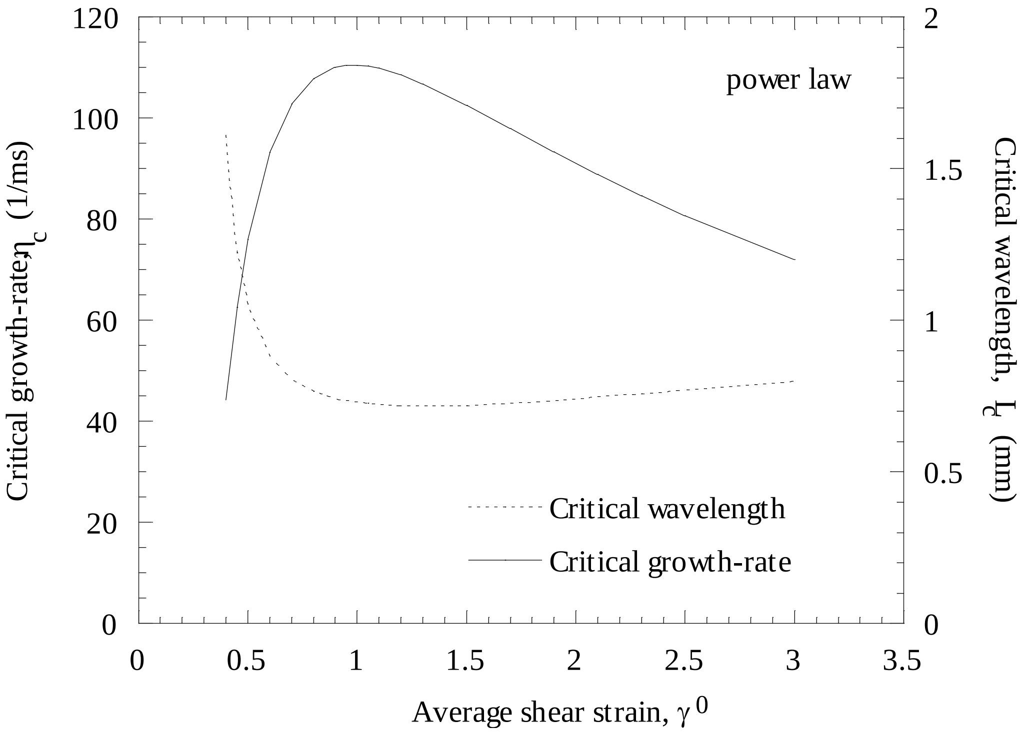

Figure 3: The dependence, on the average shear strain when the homogeneous solution is perturbed, of the critical growth rate and the critical wavelength for the power law and the MTS model.

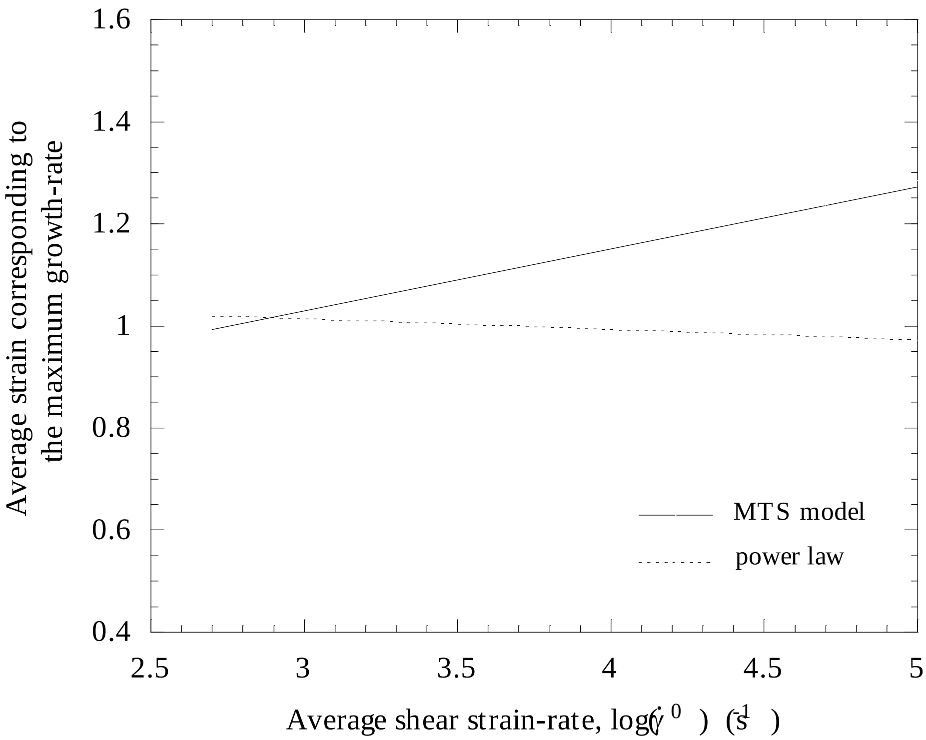

Figure 4: Dependence upon the average strain rate of the average strain corresponding to the maximum growth rate of the perturbation.

Using the definition (19), Figure 5 depicts the dependence of the shear band spacing upon the nominal strain-rate for the MTS model and the power law. For each of these models, the shear band spacing decreases rapidly with an increase in the nominal strain-rate. We note that the shear band spacing depends on the used constitutive relation and the difference between the two results reduces at high strain rates. For the nominal strain-rate of 10^4 s^{-1}, the predictions obtained here for HY-100 steel by the MTS model and the power law are respectively: L_{MTS} = 0.96659 mm, L_{PL} = 0.72843 mm. The results seem to be in an acceptable order in comparison to the value given in the literature. Indeed, for the CRS 1018 steel, a shear band spacing of 1.4 mm was reported by Molinari [11] in the some conditions. In an explosively loaded stainless steel cylinder, Nesterenko et al. [1] estimated the strain-rate within a shear band to equal 10^4 s^{-1}, and measured shear band spacing of about 1 mm. We note that the stainless mechanical properties are close to those of HY-100 steel. Our predictions using the MTS model are therefore in excellent agreement with the experimental results of Nesterenko et al.[1].

In Figure 6, we consider the variation of the shear band spacing L_s in terms of the thermal conductivity k for both the MTS model and the power law. The effect of conductivity is shown to be significant for both models. The shear band spacing L_s increases monotonically with an increase in k. This is in accord with the known stabilizing effect of the thermal conductivity. However, the shear band spacing obtained by the MTS model is larger than that obtained by the power law and the gap between the two predictions increases with thermal conductivity coefficient.

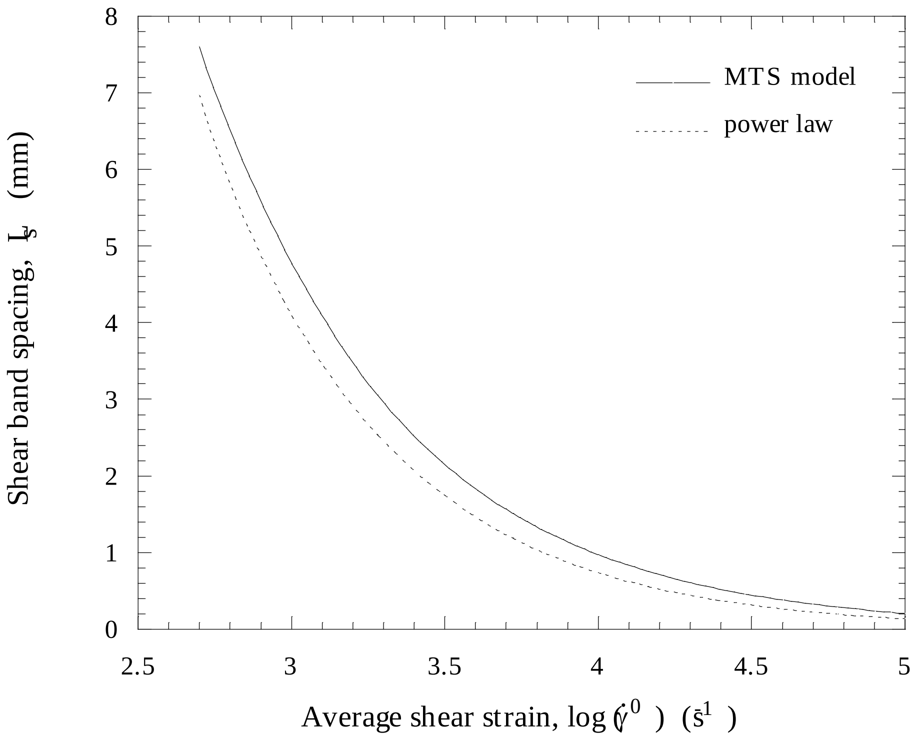

Figure 5: The variation of the shear band spacing on the average shear strain-rate, for the power law and the MTS model for HY-100 steel.

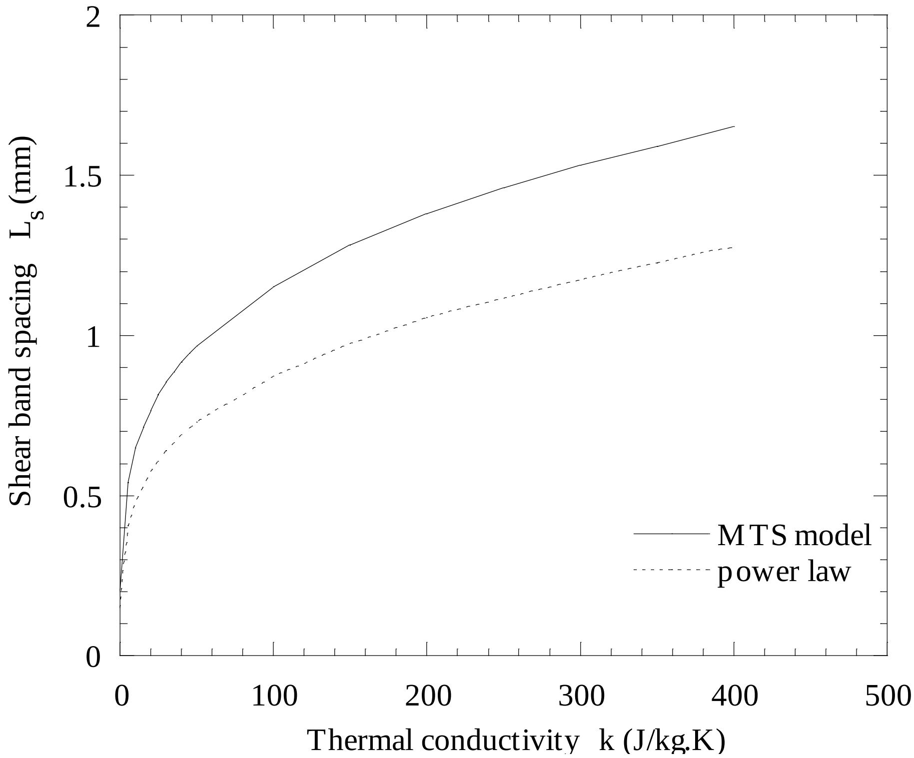

Figure 6: The variation of the shear band spacing on the thermal conductivity, for the power law and the MTS model.

6. CONCLUSIONS

We proposed the use of the MTS model along with the use of the perturbed method for analysis of shear band spacing in HY-100 steel. The MTS model describes the evolution of the flow stress based on dislocation concepts. This model provides a better description of the flow behavior for a large range of strain rates including low and high strain rates. The use of this model requires a numerical solution of the heat equation (2) and the evolution equation of the internal variable $\hat{\tau}_\varepsilon$. However, in existing works on the analysis of shear band spacing, the used models for the flow stress such as the power law lead to analytical solution of the heat equation. In order to compare to existing analyses, we used the power law model. Results from the MTS model have the same trends as the power law as well as other used models in literature. However, the predicted shear band spacing by the MTS model seems to be in a better agreement with the experimental results then that of the simple power law and other existing models. We have shown that the MTS model predicts well the value of the shear band spacing, and the influence of strain rate and thermal conductivity on the shear band spacing. Strain rate has a destabilizing effect whereas thermal conductivity has a stabilizing effect. The power law model predicts the same behavior but with a significant difference in the values of the shear band spacing.

REFERENCES

1. Nesterenko, V.F., Meyers, M.A., Wright, T.W., Collective behavior of shear bands, In: Murr, L.E., Staudhammer, K.P., Meyers, M.A. (Eds.), Metallurgical and Materials Application of

Shock-Wave and High-Strain-Rate Phenomena. Elsevier Science, Amsterdam, pp. 397-404, (1995).
2. Marchand, A., Duffy, J., An Experimental Study of the Formation Process of Adiabatic Shear Bands in a Structural Steel, J. Mech. Phys. Solids 36, pp. 251-283, (1988).
3. Grady, D.E., Kipp, M.E., The growth of unstable thermoplastic shear with application to steady wave shock compression in solids. J. Mech. Phys. Solids 35, pp. 95-118, (1987).
4. Wright, T.W., Ockendon, H., A scaling law for the effect of inertia on the formation of adiabatic shear bands. Int. J. Plasticity 12, pp. 927-934, (1996).
.5. Clifton, R.J., Adiabatic shear in material response to ultra loading rates. Report N° NMAB-356. National Advisory Board Committee, pp. 129-142 (Chapter 8), (1978).
6. Bai, Y.L., Thermo-plastic instability in simple shear. J. Mech. Phys. Solids 30, pp. 195-207, (1982).
7. Molinari, A., Instabilité thermo-visco-plastique en cisaillement simple. J. Méc. Théor. Appl., 4, pp. 659-684, (1985).
8. Molinari, A., Shear band analysis. Solid St. Phenomena 34, 447-468, 1988.
9. Shawki, T.G., Clifton, R.J., Shear band formation in thermal viscoplastic materials. Mech. Mater. 8, pp. 13-43, (1989).
10. Bai, Y.L., Dodd, B., Adiabatic shear localization: Occurrence, Theories and Applications. Pergamon Press, Oxford , (1992).
11. Molinari, A., Collective behavior and spacing of adiabatic shear bands. J. Mech. Phys. Solids 45, pp. 1551-1575, (1997).
12. Batra, R.C., Chen Li, Effect of viscoplastic relations on the instability strain, shear band initiation strain, the strain corresponding to the minimum shear band spacing, and the band width in a thermoviscoplastic material. Int. J. Plasticity 17, pp. 1465-1489, (2001).
13. Follansbee, P.S., Kocks, U.F., A constitutive description of the deformation of copper based on the use of the mechanical threshold as an internal state variable. Acta Metall. 36, pp. 81-93, (1988).
14. Mecking, H., Kocks, U.F., Kinetics of flow and strain-hardening. Acta Metall. 29, pp. 1865-1875, (1981).
15. Goto, D.M., Bingert, J. F., Chen, S. R., Gray, G. T., Garrett, R. K., The mechanical threshold stress constitutive-strength model description of HY-100 steel, Metall. Mat. Trans. Vol. 31A, pp. 1985-1996, (2000).
16. Kocks, U.F., Argon, A.S., Ashby, M.F., Thermodynamics and Kinetics of Slip. In: B. Chalmers, J.W. Christian and T.B. Massalski, Editors Prog. Mater. Sci., Vol. 19. Pergamon Press, New York, (1975).
17. Varshni, Y.P., Temperature dependence of the elastic constants. Phys. Rev. Vol. B 2, pp. 3952–3958, (1970).
18. Chen, S.R., Gray, G.T., Constitutive behavior of tantalum and tantalum-tungsten alloys, Metall and Mat Trans A, 27A, pp. 2994-3006, (1996).
19. Klopp, R.W., Clifton, R.J., Shawki, T.G., Pressure-shear impact and the dynamic viscoplastic response of metals. Mechanics of Materials 4, pp. 375-385, (1985).
20. Molinari, A., Clifton, R., Résultats exacts en théorie non liniéare. Comptes Rendus Académie des Sciences, II, pp. 1-4, (1983).
21. Batra, R.C., Kim, C.H., Effect of viscoplastic flow rules on the initiation and growth of shear bands at high strain rates. J. Mech. Solids 38, pp. 859-874, (1990).
22. Batra, R.C., Kim, C.H., Adiabatic shear banding in elastic-viscoplastic nonpolar and dipolar materials. Int. J. Plasticity 6, pp. 127-141, (1990).
23. Batra, R.C., Kim, C.H., The interaction among adiabatic shear bands in simple and dipolar materials. Int. J. Engng. Sci. 28, pp. 927-942, (1990).